MRI Birdcage Coil Design

An application note on the modelling of a 7T MRI birdcage headcoil in FEKO.

Introduction

The use of magnetic resonance imaging (MRI) in medical diagnosis continues to grow. In order to achieve better image resolution, the trend in MRI is toward higher frequencies, e.g. 300 MHz for 7 Tesla magnetic fields. At such frequencies, the RF coil radius is of the same order of magnitude as the wavelength in the human tissue. Long gone are the days when an RF coil could be designed with quasi-static techniques or by going through many cycles of prototype adjustment. Full-wave electromagnetic simulators are the backbone of RF birdcage coil design today.

Given the fact that RF MRI coils always operate at one particular frequency, it is natural to employ a frequency-domain simulation method. Two such methods are the method of moments (MoM) and the finite element method (FEM). While the MoM is efficient and accurate to solve the empty coil, or coil with a generic phantom, the hybrid MoM/FEM offers an especially useful solution for accurate simulation of MRI systems with anatomical models. The MoM is well suited to the solution of the curved metallic geometries of the coil and the FEM for the modelling of the conductive tissue in human phantoms. The finite difference time domain (FDTD) method also offers efficient solutions to coils with anatomical models due its straightforward approach to discretisation of the models and may be more suitable for those cases where the FEM memory requirements become large.

In this white paper, we demonstrate the application of both MoM and the hybrid MoM+FEM in FEKO to design RF birdcage coils.

RF Design of MRI Birdcage Coils

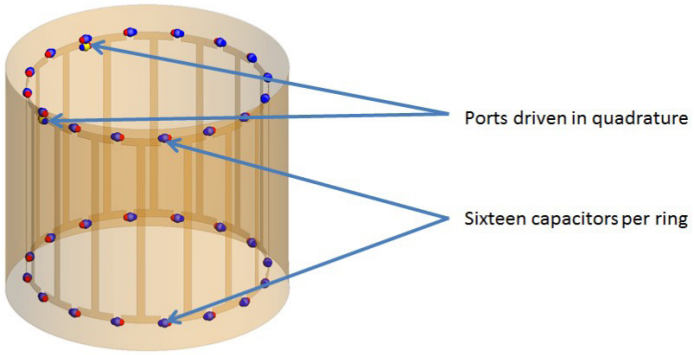

FEKO model of the 7T head coil

As an example of birdcage coil design, we use a 7T head coil based on a design in [1], shown above. In this case, 32 capacitors of 4.13 pF are used to tune the resonance at 300 MHz. The coil is excited using 2 ports; the quadrature mode is achieved with a 90 degree phase shift between the I and Q channels and simulated with the MoM. From evaluating the B1+ field of the empty coil it is clear that a good field homogeneity has been achieved for the design.

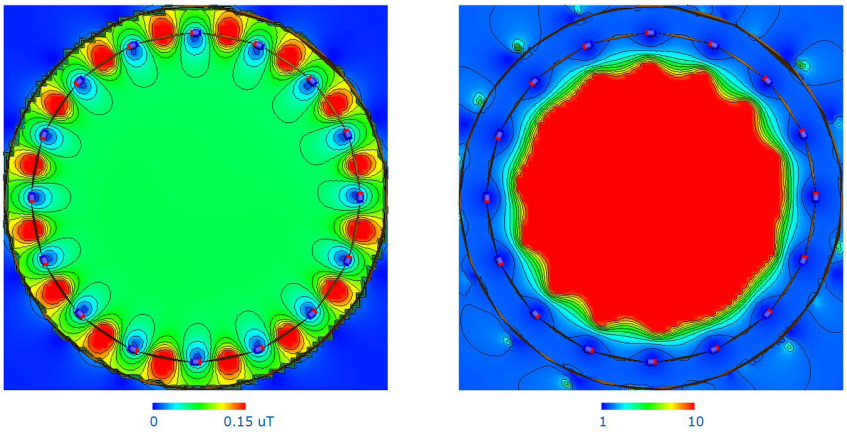

Empty coil performance at resonance: B1+ field and polarization efficiency

Addition of a Human Head Phantom

Assessing the performance of the coil with realistic loads can be carried out in two stages. Initially, homogeneous loads are employed (e.g. cylindrical, elliptical or homogeneous head phantoms), to determine the loaded performance for a well defined scenario. This stage can typically be simulated with minimum computational requirements and therefore can also be included in an optimization cycle. In the second stage, the actual performance for realistic anatomical loads is calculated. Due to the complexity of the anatomical model detail, this stage typically requires additional computational resources.

Essential for the image quality is B1+ field homogeneity in the region of interest [2, 3]. The figure below shows the B1+ field at different slices in the ROI for the simulation of the coil with the homogeneous head model is mostly between 1 and 1.5 µT in the head.

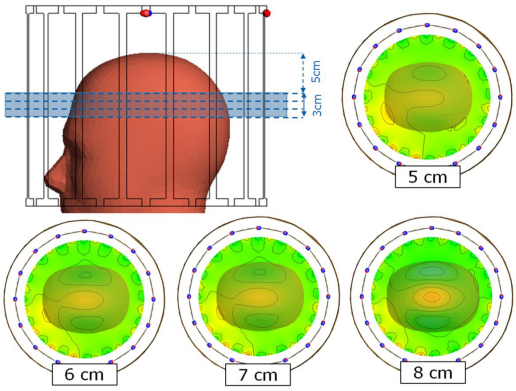

B1+ Field homogeneity in cross sections through the region of interest. Scale: linear, 0 to 2 µT with excitation 20 V per port

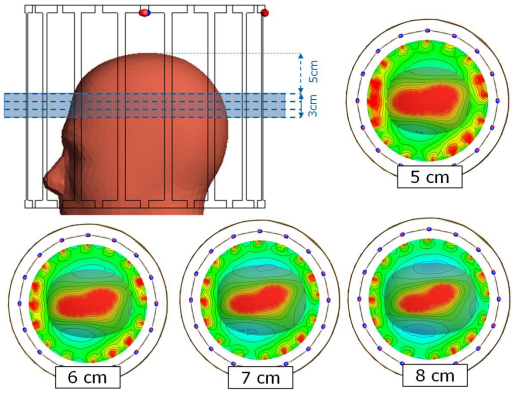

|B1+|/|B1-| ratio in cross sections through the region of interest. Scale: linear, 0 to 5

It is clear that the addition of the head somewhat degrades the homogeneity performance of the coil, with typical (at 7T) focusing of the field at the center of the head. Wang [1] goes further and includes an array of small detuned loops around the head to improve the field homogeneity in the ROI.

The homogeneous head model is then replaced by an anatomical head phantom (provided by humanbodymodels.com, a Simpleware product), which has an average tetrahedral size of 6.3 mm. The model is simulated with hybrid MoM/FEM, where the coil geometry is solved with MoM and the head model is solved with FEM. The calculated B1+ field is shown below.

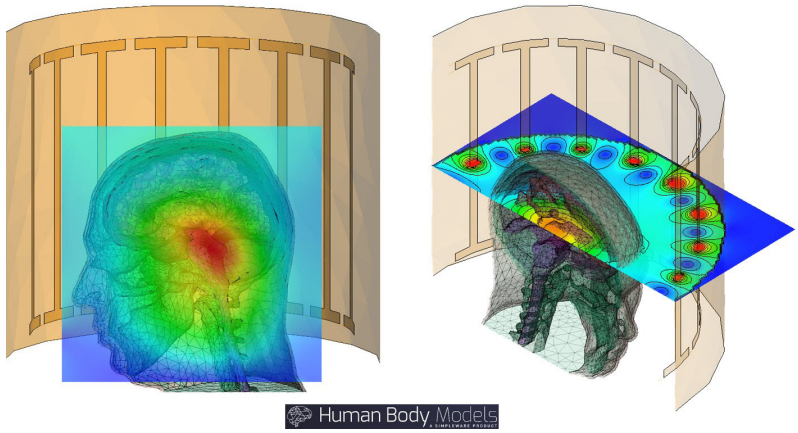

B1+ field for the coil with an anatomical head phantom

The computational requirements for the different simulations and different solvers are shown below. While all the simulations run in an acceptable time, it is clear that if automated optimization of the coil is required, then the empty coil, or coil with homogeneous load would be more suitable.

	empty coil (MoM)	coil & homogenous head phantom (MoM)	coil & anatomical head phantom (MoM+FEM)
triangles	514	4038	892
tetrahedral	-	-	132572
simulation time (min)	0.85	12	48
RAM (MB)	4	965	3309

Computational requirements for the different simulation configurations

ISNR

Another important quantity is the intrinsic signal-to-noise ratio (ISNR), which is defined in [4] as:

$$\mathrm{ISNR} = \frac{V_{\mathrm{sig}}}{V_{\mathrm{noise}}} = \frac{\omega \Delta V M_0 |B_t^-|}{\sqrt{4kT\Delta f R_L}}$$

where ω = 2πf, the Larmor frequency in rad/s, ΔV is the voxel volume, M0 is the magnetization, 0.02288 A/m (at 7T), |Bt-| is the magnitude of the anti-rotating field component used in receiving mode, k is Boltzmann's constant, 1.38E-23 J/K, T is the temperature, Δf is the bandwidth of the receiving system, RL is the noise resistance of the detector.

For the ISNR calculation a single port with a current of 1 A is used to excite the birdcage. This is easily accomplished in FEKO, since FEKO has an integrated schematic to attach transmission lines and circuits described by S-parameters or Touchstone files to the 3D model. A 90-degree hybrid is used to achieve the phase shift for the Q channel.

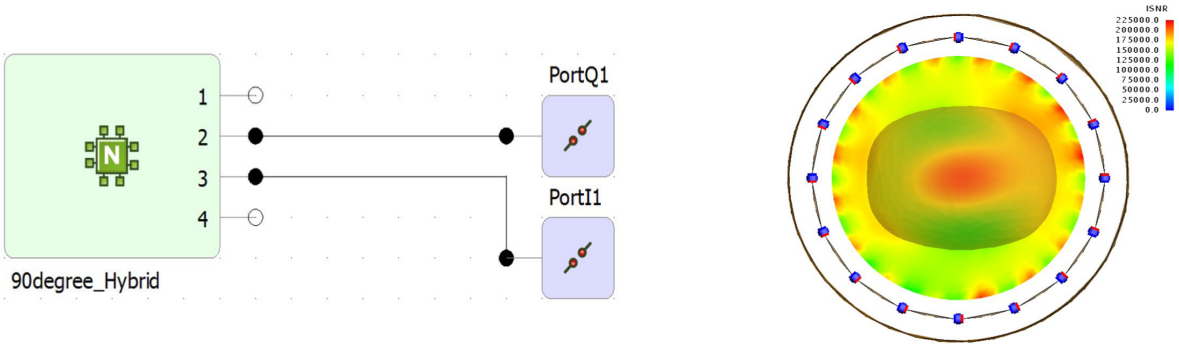

A feed circuit is easily added to the 3D model in a schematic window (left). The intrinsic signal-to-noise ratio ISNR [(√Hz)/ml] is shown (right)

The figures above shows the ISNR in a representative cross section, 7 cm below the top of the head. It was calculated with the following parameters: f=300 MHz, ΔV= 1 ml =1E-6 m3, M0 = 0.02288 A/m, T=300 K, Δf =1 Hz, RL=46.9 Ω (the latter value obtained from the FEKO simulation). It is clear that the coil has the highest ISNR at the center of the head. In general, the ISNR is good throughout the head phantom and the coil has good receive performance. The ISNR can also be useful when simulating MRI surface coil arrays.

The script used to calculate the B1+ field and ISNR can be downloaded from here.

RF Safety

Finally, MRI RF coil design is not complete without ensuring that safety standards are satisfied. With the coil in transmitting mode, we apply 20 V to both ports. The local specific absorption rate (SAR) is presented in the figure (below).

The peak 1g spatial peak averaged SAR, which is a standard FEKO output, is 0.89 W/kg in the head. This satisfies MRI safety standards [5,6].

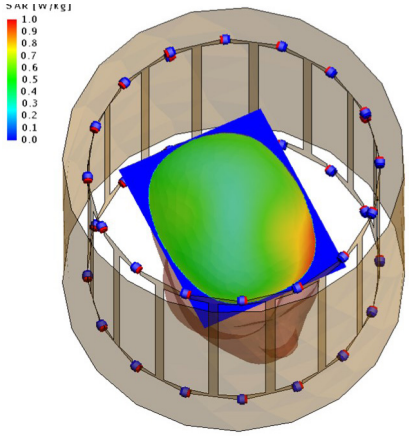

SAR distribution 7 cm below the top of the head

Conclusion

We have shown how the hybrid FEM/MoM can be used advantageously in RF coil design for MRI, using each method for those parts of the model where it performs best: FEM in a heterogeneous body phantom and MoM for the coils. MoM is very efficient for the metal coils, since the unknowns in this method are the currents on the surfaces. This contrasts with FEM and FDTD, methods in which the unknowns are the fields and therefore need to discretize the air near the metals very finely to capture the strong field gradients.

Of particular interest to the RF coil designer are homogeneity of B1+, the ratio |B1+|/|B1-|, the ISNR and the SAR, all of which are easily obtained from FEKO.

References

[1] S. Wang et al., B1 Homogenization in MRI, IEEE Trans. Medical Imaging, vol. 28, no. 4, pp. 551-554, 2009.

[2] D.I. Hoult, Sensitivity and power deposition in a high-field imaging experiment, J. Magn. Reson. Imag., vol. 12, pp. 46-67, 2000.

[3] J.P. Hornak, The Basics of MRI, http://www.cis.rit.edu/htbooks/mri, 2011.

[4] A. Kumar and P.A. Bottomley, Optimized Quadrature Surface Coil Designs, Magn. Reson. Mater. Phy., vol. 21, no. 1-2, pp. 41-52, March 2008.

[5] IEC 60601-2-33, Ed. 2.0, Medical Electrical Equipment, Part 2-33, Particular requirements for the safety of magnetic resonance equipment for medical diagnosis, 2002.

[6] R.C. Smith, R.C. Lange, Understanding Magnetic Resonance Imaging, CRC Press, Boca Raton, FL, 1998.